Simultaneous Mapping of B1 and Flip Angle by Combined Bloch-Siegert, Actual Flip-angle Imaging (BS-AFI)

Samuel A. Hurley[1], Pouria Mossahebi[2,3], Kevin M. Johnson[1], and Alexey A. Samsonov[3]

[1]*Medical Physics, University of Wisconsin, Madison, WI, United States,* [2]*Biomedical Engineering, University of Wisconsin, Madison, WI, United States,* [3]*Radiology, University of Wisconsin, Madison, WI, United States*

Introduction: The accuracy of many quantitative MRI (qMRI) methods depends critically on accurate knowledge of radiofrequency transmit field amplitude (B_1) or flip angle (FA). While the terms B_1 and FA are sometimes used interchangeably, FA depends not only on B_1 but also additional factors such as RF pulse envelope, slab profile, tissue relaxation parameters, and B_0 effects that can lead to substantial errors when correcting qMRI methods [1]. In general, B_1 correction is most appropriate for nonselective pulses (e.g. off-resonance pulse in magnetization transfer (MT) or a hard 180º pulse in inversion recovery) while FA correction is appropriate for selective excitation pulses (e.g. variable flip angle T_1 mapping). Many methods such as quantitative MT [2,3] and Look-Locker T_1 mapping utilize both types of pulses in the same experiment, however to date no consideration has been made of separate B_1 and FA effects. Therefore, the measurement and correction of both parameters may increase the overall accuracy of such methods.

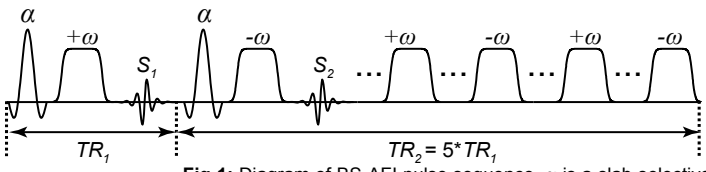

Fig 1: Diagram of BS-AFI pulse sequence. α is a slab-selective excitation pulse, while ±ω is a nonselective Fermi pulse applied at ±ω Hz with respect to center frequency. Additional Fermi pulses continue to play at regular intervals during the second TR (figure compressed to save space).

Bloch-Siegert B_1 mapping (BS) is a recently proposed phase-based method to rapidly map B_1 with an off-resonant nonselective pulse [4], while Actual Flip-angle Imaging (AFI) is a method to map FA using the ratio of signals from two interleaved steady-state TRs [5]. We propose a novel combination of these two sequences, BS-AFI, to map FA using image magnitude and encode B_1 into the image phase with zero time penalty over AFI. Improved MT accuracy is demonstrated in phantom validations.

Methods: The BS-AFI pulse sequence was implemented on a GE MR750 (fig. 1). A standard AFI pulse sequence was implemented by the addition of a second TR_2 (=5*TR_1) to an SPGR sequence; BS mapping was then added through the introduction of an 8ms Fermi-shaped off-resonance pulse just after the excitation pulse and just before phase encoding. As BS requires the phase differences of two ±ω off-resonance pulses, a pulse at +4kHz is played during TR_1 and -4kHz during TR_2. Four additional alternating pulses are played during TR_2 to maintain a pulsed steady-state saturation. A potential issue of this implementation is if MT saturation effects are different between TR_1 and TR_2 due to variation is center frequency with B_0. However, since the TR of the AFI sequence is shorter than the timescale of MT exchange, we hypothesize that these alternating pulses will create an averaging effect and generate the same MT contrast in both images, eliminating any confounds to AFI quantification. The B_1-dependant phase precession may also interfere with RF spoiling, however it was shown that the use of large spoiler gradients eliminates sensitivity to RF spoiling effects [6].

A cylindrical gelatin phantom was scanned at 64x48x52 matrix and 1.5^3 mm^3 isotropic resolution in the coronal plane, then re-formatted to axial to visualize slab profile (vertical direction). BS-AFI and standard AFI scans were acquired with TR_1/TR_2 = 36/180ms and α = 55º. Spoiled gradient echo (SPGR) scans were acquired with TR = 36ms and α = [5 10 20 30 40]º. Ten MT-weighted SPGR were acquired with TR = 36ms, α = 10º, and offset frequency Δ = [1 2.5 4 9 13] kHz for MT flip angles 500º and 920º. The SPGR and MT data were then fitted to a five-parameter model of MT (bound pool fraction, exchange rate, T_2 of bound pools, *PD*, and T_1 of free pool) [7]. The qMT data were corrected in three ways: using only the FA map to correct both excitation and MT pulse flip angles (FA only), using only the B_1 map to correct both (B_1 only), and using the BS-AFI FA to correct the excitation flip angle and B_1 to correct MT flip angle. B_0 correction was done using IDEAL [8].

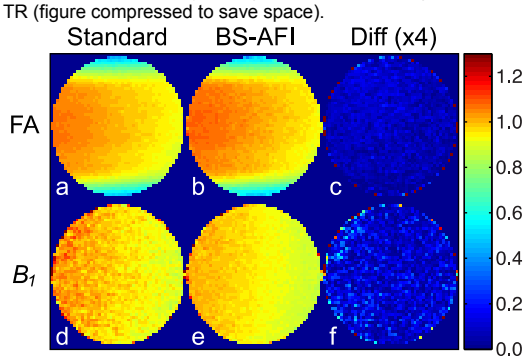

Fig 2: Comparison of standard AFI (a) & BS (d) methods to the combined BS-AFI approach (b,e), normalized by nominal flip angle. Significant differences between FA (a,b) and B_1 (d,e) are observed, primarily due to slab profile (vertical direction). Absolute error (c,f) is quite uniform, despite large off-resonance within slice (~200 Hz, not shown).

Results: Mean error for the BS-AFI method, compared to separate AFI and Bloch-Siegert mapping, was 3.0 ± 2.2% in B_1 and 2.0 ± 1.1% in FA (fig. 2). Spatially varying differences between techniques were not observed, even in the presence of B_0 inhomogeneity (0–200 Hz within slice, as measured with IDEAL). SNR of the B_1 map was also improved (variance $\sigma_{STANDARD}$ = 0.0048 G, $\sigma_{BS\text{-}AFI}$ = 0.0037 G; small ROI in center of image) due to increased signal from a longer AFI TR_2. qMT parameter maps using only FA or B_1 show distinct errors due to slab profile (fig. 3, see caption). BS-AFI maps show uniform measures along the slab direction (fig. 4).

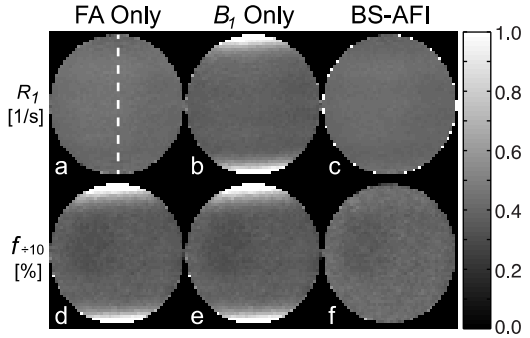

Fig 3: R_1 (=1/T_1) (a-c) and bound pool fraction *f* (d-f) maps using three correction approaches. Note that R_1 mapping using B_1 correction (b) or correction of MT pulse with FA (d) both result in large residual errors due to slab profile. Similar errors were observed in PD and exchange rate (not shown).

Discussion & Conclusions: Simultaneous knowledge of B_1 and FA may be useful for a wide range of qMRI applications that employ both selective and non-selective RF pulses, including quantitative MTI, Look-Locker T_1 mapping, and the correction of stimulated echoes in a multi-exponential T_2 CPMG experiment [9]. Although errors in FA due to slab profile can be minimized in other ways, such as the use of a longer optimized RF pulse or nonselective 3D imaging, such approaches are not always feasible. Nonselective imaging is only acceptable in applications where the object is sufficiently small to be covered by two phase encoding directions in a reasonable scan time, and may lead to additional errors due to increased sensitivity to B_0 variations. Pulses that are optimized for slab selection may still have residual errors in a significant number of slices, as we have observed errors greater than 5% in quantitative maps occur in 1/3 of our slices. These approaches also do not consider variations in FA due to B_0 or the relaxation properties of tissue (e.g. T_2 relaxation in ultrashort TE sequences).

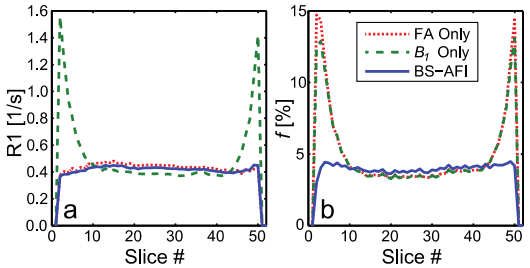

Fig 4: Plot of R_1 and *f* along slab profile (dash line in fig. 3a).

In contrast, the BS-AFI method enables rapid and accurate qMRI with sequences employing any combination of selective or non-selective RF pulse types. The key feature of the pulse sequence is encoding the two alternating off-resonance shifts into two AFI TRs. This may potentially influence contrast of AFI images differently if TR is long, however no variations were observed in our experiment using typical AFI parameters. [3,6]. This averaging effect may be beneficial not only in the context of BS-AFI, but also B_0-insensitive qMT or MT ratio measurements, and will be the subject of future work. In conclusion, we present a method to simultaneously map B_1 and FA that is robust to B_0 and MT errors and incurs no scan time penalty over the traditional AFI method. In context of MT, separate measurement of FA for excitation flip angle correction and B1 for MT power correction led to a significant increase in the accuracy of bound pool fraction. In addition to enlongated scan times, separate acquisition of such maps may result in reduced consistantcy of B_1 and FA mapping due to patient motion.

References: [1] Wang et al. MRM 2006;56:463 [2] Sled JG et al. MRM 2001;46:923 [3] Yarnykh VL MRM 2002;47:929 [4] Sacolick, LI et al. MRM 2010;63:1315 [5] Yarnykh VL MRM 2007;57:192. [6] Yarnykh VL MRM, 2010;63:1610 [7] Mossahebi P et al. WMSG 2011 p13. [8] Yu, H. JMRI 2007;26:1153 [9] Prasloski T. et al. MRM 2011 (in press). **Acknowledgements**: We acknowledge the financial support of the NIH (NINDS R01NS065034).